3D PRINTING AND ADDITIVE MANUFACTURING
Volume 7, Number 3, 2020

DOI: 10.1089/3dp.2019.0129

ORIGINAL ARTICLE

Three-Dimensional Printed Stamps for the Fabrication of Patterned Microwells and High-Throughput Production of Homogeneous Cell Spheroids

Tomas Gonzalez-Fernandez,[1] Alejandro J. Tenorio,[1] and J. Kent Leach[1,2]

Abstract

Aggregation of cells into spheroids and organoids is a promising tool for regenerative medicine, cancer and cell biology, and drug discovery due to their recapitulation of the cell–cell and cell–matrix interactions found *in vivo*. Traditional approaches for the production of spheroids, such as the hanging drop method, are limited by the lack of reproducibility and the use of labor-intensive and time-consuming techniques. The need for high-throughput approaches allowing for the quick and reproducible formation of cell aggregates has driven the development of soft lithography techniques based on the patterning of microwells into nonadherent hydrogels. However, these methods are also limited by costly, labor-intensive, and multistep protocols that could impact the sterility of the process and efficiency of spheroid formation. In this study, we describe a one-step method for the fabrication of patterned nonadherent microwells into tissue culture plates using three-dimensional (3D) printed stamps and evaluate the production of cell spheroids of different sizes and cell sources. The generation of bone marrow-derived mesenchymal stromal cell and endothelial cell spheroids by the use of 3D printed stamps was superior in comparison with a widely used multistep mold technique, yielding spheroids of larger sizes and higher DNA content. The 3D stamps produced spheroids of more consistent diameter and DNA content when compared with other commercially available methods. These 3D printed stamps offer a tunable, simple, fast, and cost-effective approach for the production of reproducible spheroids and organoids for a wide range of applications.

Keywords: 3D printing, microwell, cell spheroids, 3D cell culture methods, micropatterning

Introduction

THE *IN VITRO* AGGREGATION OF CELLS into three-dimensional (3D) spherical structures aims to better recapitulate the *in vivo* complexity of tissues and organs compared with cells in monolayer culture. Cells aggregated into spheroids mimic *in vivo* cell–cell and cell–matrix interactions and offer increased cell viability by promoting cellular communication and signaling pathways.[1–3] In light of these advantages, the production of cell spheroids has been explored for different applications such as enhanced tissue regeneration,[4–6] the engineering of 3D self-organized organ models (also known as organoids),[7] the investigation of embryonic development[8] and cancer processes,[9] and as tools for pharmacological discovery.[10]

The first reported fabrication method for the 3D aggregation of cells was the hanging drop method,[11] which consists of the spontaneous aggregation of dispersed cells contained in inverted drops. After this finding, other techniques based on cell self-aggregation such as spinner flask culture,[12] static liquid overlay,[13,14] cell centrifugation,[15] and magnetic levitation[16] were developed. Although these methods are effective at producing spherical cell aggregates, the resultant spheroids have increased variability and low reproducibility. In addition, these techniques can compromise cell viability due to high shear stresses, are labor-intensive, and require additional handling after spheroid production.[17] The need for consistent high-throughput production of cell spheroids and organoids has fostered the investigation of new cell

[1]Department of Biomedical Engineering, University of California, Davis, Davis, California, USA.
[2]Department of Orthopaedic Surgery, School of Medicine, UC Davis Health, Sacramento, California, USA.

aggregation methods such as those based on micromolded nonadhesive hydrogel microwells.[17,18]

A variety of techniques have been explored to produce microwells such as soft lithography and photopolymerization. Poly(dimethylsiloxane) (PDMS) molds were surface-modified through either hexa(ethylene glycol)-terminated self-assembled monolayers or bovine serum albumin to pattern the surface of gelatin, agarose, and Matrigel hydrogels.[19] Microstructures were also generated through photopolymerization with methacrylated hyaluronic acid by introducing a photoinitiator to the hydrogel and providing posterior exposure to UV light while casted on a PDMS mold.[20] The resulting microwells facilitated the formation of embryonic cell spheroids, yet the consistency in spheroid shape and size was not assessed.[20] The two aforementioned methods are limited by labor-intensive multistep protocols that require the use of toxic chemicals that could affect spheroid viability and cumbersome sterilization procedures that compromise the use of these systems for experiments requiring cell culture for prolonged periods of time. In addition, these methods require the photolithographic production of a photosensitive epoxy resin master mold using photomasks, which is a costly and time-consuming process.[21]

The use of commercially available nonadhesive micropatterned plastic well plates has been proposed as an alternative to these techniques, but the high costs and suggested one-time use hinders their adoption in many laboratories.[22] Recently, 3D printing technology has been employed for rapid prototyping of 3D objects in a precise and cost-effective manner. Despite the advantages offered by 3D printing, it remains relatively unexplored for the fabrication of devices that facilitate the production of microwells for cell aggregation. Mehesz *et al.* described the use of a 3D printed 96 pillar mold resembling the dimensions of a 96-well plate but including 61 micropillars per pillar to cast rounded bottom microwells into agarose gels for cell aggregation.[23] Although these microwells outperformed the hanging drop method, this approach is limited to the formation of aggregates of reduced dimensions and cell numbers, and its combination with a robotic automated system for optimal performance limits its adoption by many laboratories. Therefore, the development of new devices that allow for the cost-effective production of spheroids of different sizes and cell types is still needed.

Recently, our laboratory reported a simple protocol using micropatterned positive silicon molds to produce microwells in agarose hydrogels that can easily be inserted into tissue culture plates for the formation of stem cell spheroids.[24] Despite offering a rapid and cost-effective alternative to the previously mentioned techniques, the production of hydrogels and their subsequent transfer to a culture plate could negatively impact their sterility and result in inefficient cell seeding onto the microwells due to poor fit of the hydrogel to the borders of the culture well. To address these challenges, we designed a 3D printed stamp system for the rapid *in situ* production of reproducible microwells directly into 24-well plates. The method reported in this study describes the use of these 3D printed stamps for the formation of homogeneous spheroids of different sizes and cell sources to facilitate the consistent high-throughput production of spheroids.

Materials and Methods

Stamp design and 3D printing

The stamp prototype was designed using SolidWorks 2017 software and converted into a .stl file. The design (Fig. 1A, B) consisted of (1) 29 pyramidal microwell protrusions ($S = 2$ mm, $H = 2.5$ mm) for the imprinting of the microwells into the agarose gel, (2) a tubular post ($D = 15.6$ mm, $H = 13.5$ mm) for the insertion of the stamp into the culture plate well with channels to facilitate air displacement and avoid air bubble formation during the addition of agarose into the well, and (3) a stamp stopper ($S = 17.5$ mm, $H = 9$ mm) to place and maintain the stamp at a defined height over the culture plate surface during the microwell formation process and to facilitate the stamp handling and extraction after microwell formation. The .stl file was printed in the UC Davis Translating Engineering Advances to Medicine laboratory using a Carbon M2 3D printer (Carbon, Redwood city, CA) and a urethane methacrylate resin (UMA 90) (Carbon). The printing was performed at standard resolution in a total time of 1 h for 24 stamps. After the printing process, the stamps were collected (Fig. 1C–E) and rinsed in isopropanol (Sigma Chemical, St. Louis, MO) under agitation for 15 min, left to dry at room temperature for 20 min, and UV cured for 1 min per side.

Stamp sterilization

The stamps were sterilized in ethylene oxide (EtO) using an EtO sterilization chamber (Andersen Sterilizers, Haw River, NC) and a 24 h sterilization cycle 48 h before stamp use for the fabrication of the agarose microwells. After cycle completion, the stamps remained inside the fume hood for 24 h to allow for complete EtO desorption.

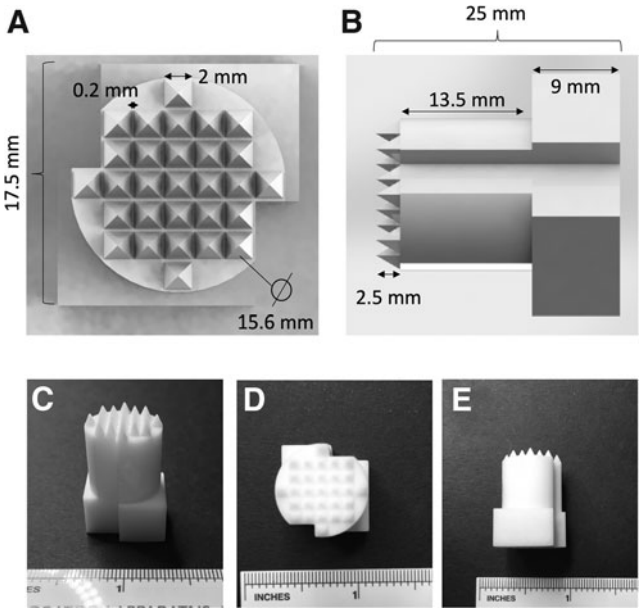

FIG. 1. Stamp design and macroscopic appearance. **(A)** Top view and **(B)** side view of the designed .stl file. **(C)** Macroscopic appearance of the 3D printed stamp prototypes formed from a urethane methacrylate resin, **(D)** top view and **(E)** side view. 3D, three-dimensional.

Agarose microwell fabrication

A 1.5% agarose (Invitrogen, Carlsbad, CA) gel solution was prepared in deionized water and autoclaved at 250°C for 1 h. After the agarose was fully dissolved, the agarose microwells were fabricated in sterile conditions (Fig. 2). First, the stamps (multiple stamps were used simultaneously to minimize the fabrication time) were inserted into the wells of 24-well tissue culture-treated culture plate (Falcon, Corning, NY) (Fig. 2A, B). Then, melted 1.5% agarose (70–90°C) was pipetted (550 μL) into the well using the stamp guide channels to allow for air displacement and avoid the formation of air bubbles (Fig. 2C). The agarose was allowed to gel at room temperature for 5 min (Fig. 2D), and the stamp was manually extracted from the well using the stamp stopper (Fig. 2E).

We compared the efficiency of the agarose stamps with a previously described method reported by our laboratory.[5,24] This method consisted of the fabrication of patterned 1.5% agarose microwells (same dimensions as the microwells produced through the stamps) using a silicon master mold produced as previously described.[22] After gelation, agarose microwells were transferred from the mold into a 24-well tissue culture-treated culture plate.

After production of the agarose microwells, 1 mL of sterile phosphate-buffered saline (PBS) (Thermo Fisher Scientific, Waltham, MA) was added into the wells, and the plates were centrifuged for 8 min at 900 rpm. After centrifugation, PBS was aspirated to remove any free agarose, and 1 mL of fresh sterile PBS was added to keep the microwells hydrated until cell seeding.

Bone marrow-derived mesenchymal stromal cell and endothelial cell culture

Human bone marrow-derived mesenchymal stromal cells (MSCs) from a single donor were purchased from Lonza (Walkersville, MD). MSCs were expanded under standard conditions until use at passages 4 – 6 in growth medium containing minimum essential alpha medium (w/L-glutamine, w/o ribo/deoxyribonucleosides; Invitrogen) supplemented with 10% fetal bovine serum (Atlanta Biologicals, Atlanta, GA) and 1% penicillin (10,000 U/mL) and streptomycin (10 mg/mL) (Gemini Bio-Products, West Sacramento, CA). Media was refreshed every 2–3 days.

Human cord blood-derived endothelial colony forming cells (ECs) were kindly provided by Professor Eduardo Silva (UC Davis). ECs were isolated from human umbilical cord blood obtained from the UC Davis Umbilical Cord Blood Collection Program within 12 h of collection following protocols as previously described.[25] ECs were used at passages 4–6 in Endothelial Growth Media-2 Microvascular (Lonza) and supplemented with gentamycin (50 μg/mL) and amphotericin B (50 ng/mL) (PromoCell, Heidelberg, Germany).

MSC and EC spheroid formation and culture

After reaching confluency, ECs and MSCs were trypsinized with Trypsin-EDTA (0.25%) (Thermo Fisher Scientific), counted using trypan blue exclusion staining with a Countess II automatic cell counter (Thermo Fisher Scientific) and resuspended in fresh media to an appropriate volume. One microliter of the cell suspension containing 1.45×10^5 cells for the 5000 cell/spheroid group, 4.35×10^5 cells for the 15,000 cells/spheroid, and 1.31×10^6 cells for the 45,000 cells/spheroid was pipetted into the each well of the 24-well plate containing the agarose microwells. After pipetting, the plates were centrifuged at 163 *g* for 8 min and kept at 37°C and 20% O_2 for 7 days, changing the media every 2–3 days.

Assessment of MSC and EC spheroid formation

After 2 and 7 days of spheroid formation, MSC and EC spheroids were imaged using a brightfield microscope. Images were taken (6 wells per group, 4–6 images per well) and the spheroid diameter was calculated using ImageJ software. To analyze the DNA content, media was aspirated, and the spheroids were washed in PBS and collected from the wells. Spheroids were lysed in passive lysis buffer (Promega, Madison, WI), sonicated, and evaluated for total DNA content per well using a PicoGreen Quant-iT PicoGreen DNA Assay Kit (Invitrogen). For comparison between the 3D printed stamps, Aggrewell™, and the hanging drop method, single

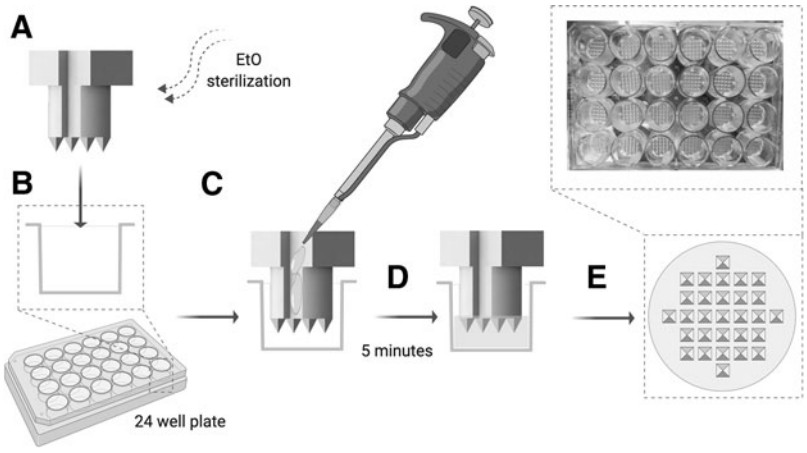

FIG. 2. Agarose microwell fabrication process. **(A)** Sterilization of the stamp, **(B)** insertion of the stamp into a 24-well tissue culture plastic well, **(C)** pipetting of the melted 1.5% agarose into the well using the stamp channels to guide the agarose pipetting and allow for air displacement, **(D)** agarose gelation for 5 min at room temperature, and **(E)** removal of the stamp using the stamp stopper at the top to obtain patterned agarose microwells. Figure created with BioRender.

spheroids from the microwells were collected, lysed, and the DNA content per spheroid was quantified.

MSC spheroid formation in commercially available systems

Aggrewell plates (STEMCELL® Technologies, Vancouver, Canada) and Perfecta3D® hanging drop plates (Sigma) were prepared and seeded according to manufacturer. For Aggrewell plates, the wells were rinsed with antiadherence rinsing solution (STEMCELL Technologies) and washed with fresh growth media. Aggrewell plates were also tested without antiadherence rinsing solution.

Statistical analysis

Statistical analyses were performed using GraphPad Prism version 8 software (GraphPad, La Jolla, CA). Statistical differences between groups were determined by a Student's *t*-test. Numerical and graphical results are displayed as mean ± standard deviation. Significance was accepted at a level of $p < 0.05$. Sample size (n) is indicated within the corresponding figure legends.

Results

3D printed stamps enable consistent formation of spheroids of different sizes

We produced spheroids of different sizes (5000, 15,000, and 45,000 cells/spheroid) from two cell sources (human MSCs and ECs). The efficiency of the stamp method was directly compared with a mold-based technique used broadly in our laboratory.[5,24] MSC spheroids (Fig. 3) produced with the stamp method resulted in spheroids of 15,000 and 45,000 cells/spheroid with a significantly larger diameter (373.0 ± 12.9 μm for the 15,000 cells/spheroid group and 582.2 ± 6.8 μm for the 45,000 cells/spheroid group) (Fig. 3A, B) compared with spheroids generated using agarose molds (354.0 ± 15.5 μm, $p = 0.044$ for the 15,000 cells/spheroid group and 571.4 ± 11.4 μm, $p = 0.042$ for the 45,000 cells/spheroid group). DNA analysis of the spheroids after collection showed significantly higher DNA content in the spheroids produced with the stamps in all spheroid sizes (Fig. 3C). Similar results were observed using ECs to produce spheroids of 5000, 15,000, and 45,000 cells/spheroid (Fig. 4). The average diameter of EC spheroids produced in the stamps (143.5 ± 5.3 μm for the 5000 cells/spheroid group, 199.6 ± 6.8 μm for the 15,000 cells/spheroid group and 282.6 ± 14.4 μm for the 45,000 cells/spheroid group) was significantly larger than those produced in the molds (111.2 ± 7.7 μm, $p < 0.0001$ for the 5000 cells/spheroid group, 170.9 ± 7.8 μm, $p < 0.0001$ for the 15,000 cells/spheroid group, and 251.4 ± 17.9 μm, $p = 0.0077$ for the 45,000 cells/spheroid group) (Fig. 4A, B). Similarly, DNA content of the 15,000 cells/spheroid and 45,000 cells/spheroid groups produced in the stamps was significantly higher (748.8 ± 97.4 ng of DNA/well for the 15,000 cells/spheroid group and 1491.0 ± 290.4 ng of DNA/well for the 45,000 cells/spheroid group) than those produced in the molds (572.2 ± 61.2 ng of DNA/well, $p = 0.0037$ for the 15,000 cells/spheroid group and 827.0 ± 325.8 ng of DNA/well, $p = 0.0039$ for the 45,000 cells/spheroid group) (Fig. 4C).

Cell seeding is more efficient in stamp-fabricated microwells

In light of increased DNA content in spheroids formed using the stamps, we investigated potential contributions to increased efficiency in spheroid production compared with mold-fabricated microwells. We formed spheroids of 15,000 MSCs/spheroid using both methods (Fig. 5A), and we

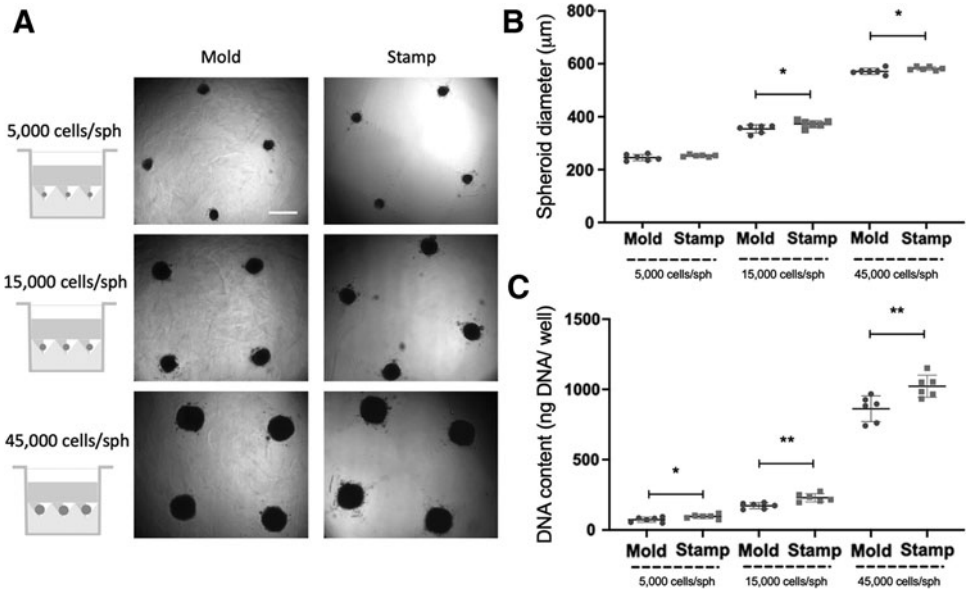

FIG. 3. Comparison of MSC spheroid formation using mold-based (Mold) and the 3D printed stamp method (Stamp). **(A)** Microscopic images of the spheroids at 48 h after cell seeding. Scale bar represents 500 μm. **(B)** Spheroid diameter (μm) after 48 h of spheroid formation using both microwell production methods. **(C)** DNA content (ng DNA per well) after 48 h of spheroid formation using both microwell production methods. *$p < 0.05$; **$p < 0.01$, $n = 6$ per group. MSC, mesenchymal stromal cell.

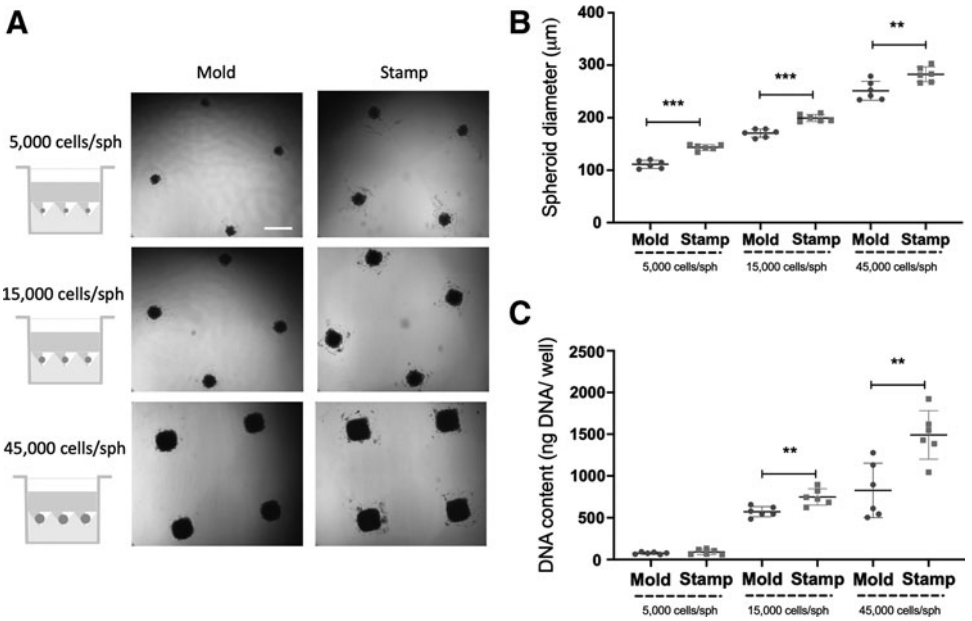

FIG. 4. Comparison of EC spheroid formation using mold-based (Mold) and the 3D printed stamp method (Stamp). **(A)** Microscopic images of the spheroids at 48 h after cell seeding. Scale bar represents 500 μm. **(B)** Spheroid diameter (μm) after 48 h of spheroid formation using both microwell production methods. **(C)** DNA content (ng DNA per well) after 48 h of spheroid formation using both microwell production methods. $^{**}p < 0.01$; $^{***}p < 0.001$, $n = 6$ per group. EC, endothelial colony forming cell.

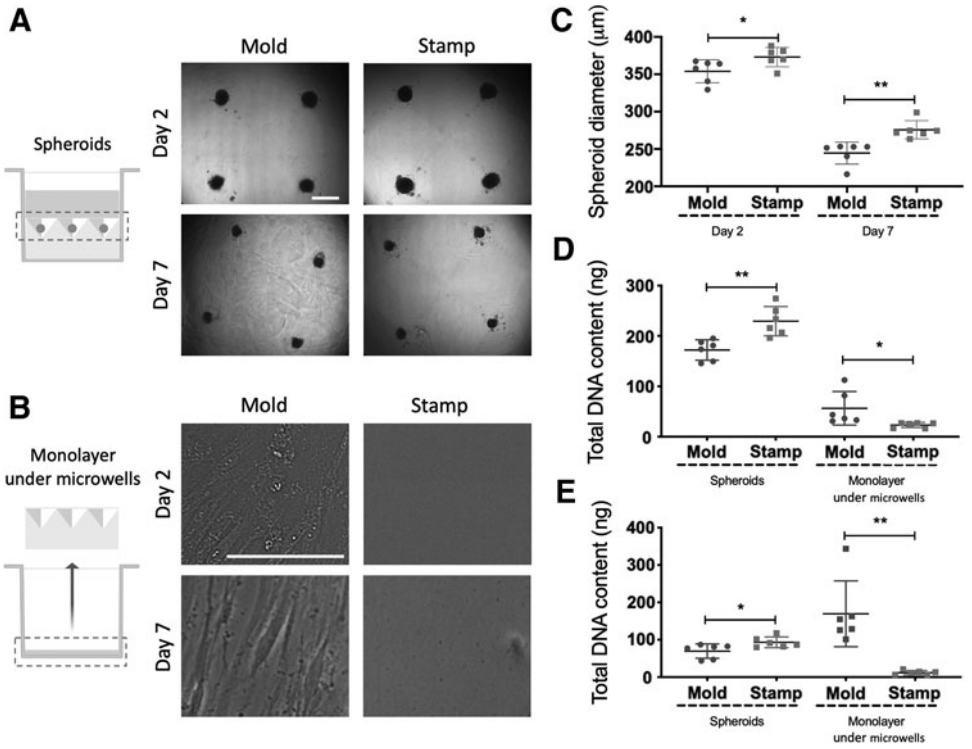

FIG. 5. Comparison of MSC spheroid formation (15,000 cells/spheroid) and maintenance in culture for 7 days when using mold-based (Mold) and the 3D printed stamp method (Stamp). **(A)** Microscopic images of the spheroids at 2 and 7 days after cell seeding. Scale bar represents 500 μm. **(B)** Microscopic images of the cell monolayer under the microwells at days 2 and 7 after cell seeding. Scale bar represents 100 μm. **(C)** Spheroid diameter (μm) after 2 or 7 days of spheroid formation using both microwell production methods. **(D)** DNA content of the spheroids and cell monolayers beneath the micropatterned molds at day 2 after spheroid production. **(E)** DNA content (ng) of the cell spheroids and cell monolayers beneath the micropatterned molds at day 7 after spheroid production. $^{*}p < 0.05$; $^{**}p < 0.01$, $n = 6$ per group.

analyzed the formation of the cell monolayer beneath the agarose microwells. No cell monolayer formation was observed under the stamp-produced agarose microwells at day 2 after spheroid formation. However, adherent cells were readily observed on the tissue culture plastic beneath the mold-fabricated microwells at day 2, which grew into a confluent cell monolayer by day 7 (Fig. 5B). Spheroid diameter was greater in spheroids produced using the stamp compared with the mold at days 2 and 7 (Fig. 5C), suggesting that cell incorporation was more efficient for stamp-produced spheroids. To confirm this observation, we measured the DNA content of the cell monolayer under the agarose microwells at days 2 and 7 after spheroid production (Fig. 5D, E), which revealed significantly higher DNA content at both time points on the plastic surfaces beneath the mold-fabricated microwells. These results confirm that cell seeding onto stamp-fabricated microwells is more efficient, blocking the escape of cells to the underlying plastic surface due to the tighter fitting of the agarose mold into the wells as a consequence of *in situ* mold production, resulting in spheroids of higher cellularity.

3D printed stamps outperform other established techniques

To assess the performance of the 3D printed stamps in comparison with other established techniques, MSC spheroids of different sizes (5000 cell/spheroid, 15,000 cells/spheroid, and 45,000 cells/spheroid) were produced using 3D printed stamps, Aggrewell wells, and the Perfecta3D hanging drop plates. Although the 3D printed stamps and the hanging drop method produced spheroids of the three different sizes, the Aggrewell plates only allowed for the production of spheroids of 5000 and 15,000 cells/spheroid, whereas the cells seeded in the 45,000 cells/spheroid aggregated into a macroscopic cell mass (Fig. 6A). In addition, spheroid–spheroid aggregation and MSCs adhesion to the surface of the Aggrewell wells were observed regardless of treatment with STEMCELL Technologies antiadherence rinsing solution (Fig. 6A). To further compare the efficacy of these three methods, the size and the DNA content of spheroids containing 15,000 cells/spheroid were analyzed after production using all three methods. Spheroids produced by the 3D printed stamps exhibited comparable diameters and DNA content to the commercially available methods with reduced variability (1.3 ± 0.3 ng of DNA/spheroid for the stamps versus 6.8 ± 4.7 for the Aggrewell and 0.9 ± 0.6 for the hanging drop method), leading to the formation of more homogeneous spheroids (Fig. 6B, C). Spheroids produced in the Aggrewell wells possessed significantly higher DNA content than spheroids produced by the hanging drop method and the 3D printed stamps ($p = 0.005$ and $p = 0.010$, respectively), but this difference and the high variability between

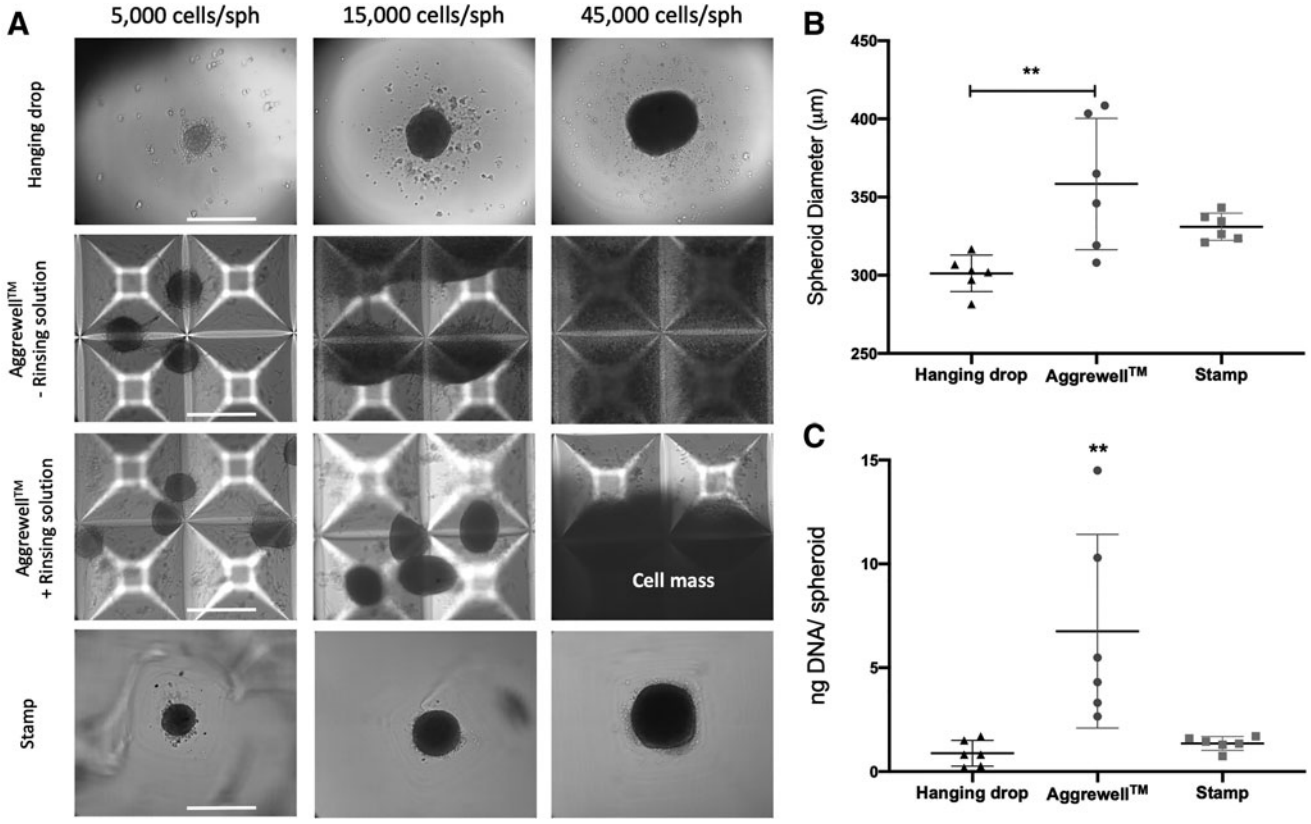

FIG. 6. Comparison of MSC spheroid formation using the 3D printed stamp method (Stamp) with other commercially available tools. **(A)** Microscopic images of MSC spheroids of different sizes (15,000, 5000, and 45,000 cells/spheroid) produced using the Perfecta3D® hanging drop system, untreated Aggrewell™ wells or wells treated with antiadherence rinsing solution, and the 3D printed stamp. Scale bar represents 500 μm. **(B)** Spheroid diameter (μm) after 48 h of spheroid (15,000 cells/spheroid) formation using the three different systems. **(C)** DNA content (ng per spheroid; 15,000 cells/spheroid) after 48 h of spheroid formation using the three different methods. $^{**}p < 0.01$, $n = 6$ per group.

spheroids were probably due to spheroid aggregation as revealed by microscopic evaluation (Fig. 6A).

Discussion

Cellular aggregates have become a powerful research tool in many laboratories, motivating the critical need for the development of reliable and cost-effective methods for their rapid and consistent production for various applications. For example, our laboratory has explored the use of MSC spheroids entrapped in instructive biomaterials to enhance the healing of skin wounds[26] and the regeneration of bone segmental defects.[5] Others have used cell spheroids and organoids for modeling the tumor microenvironment,[27] embryonic development,[28] and drug discovery.[29] In this study, we describe the engineering of a stamp for the patterning of microwells on agarose hydrogels and the subsequent use of these microwells for the formation of cell spheroids of different sizes and cell sources. The described method is superior to a silicon mold-based technique previously reported by our laboratory,[24] producing human MSC and EC spheroids with larger spheroid diameters and increased DNA content. In addition, we observed that *in situ* microwell formation within the culture plate resulted in more efficient cell seeding on the stamp-produced microwells, preventing escape of cells from the micropatterned microwells onto the underlying culture plastic plate. When compared with the commercially available Aggrewell and Perfecta3D hanging drop systems, the 3D printed stamps achieved more reproducible production of spheroids for three different cell densities and diameters.

MSC spheroids are of special relevance due to their anti-inflammatory effects,[30] increased tissue regeneration[1] and angiogenic potential,[31] improved viability and engraftment,[5] ability to facilitate MSC differentiation into multiple lineages,[32,33] and delayed senescence.[3,32] Similar to MSC spheroids, EC spheroids promote enhanced capillary formation,[34,35] cell viability,[36] and offer a promising tool for the study of tissue and tumor angiogenesis.[37,38] For all of these applications, the development of methods that provide rapid, consistent, and reproducible formation of spheroids of different cell types and sizes is needed.

Commercially available systems such as the STEMCELL Technologies Aggrewell plates and the Sigma Perfecta3D system provide ready-to-use plastic culture plates of different sizes and microwell formats in an effort to facilitate the high-throughput production of cell spheroids and organoids. However, despite the ease of use of these systems, their high commercial costs, limited capacity for the production of spheroids of different sizes and cell numbers, necessary antiadherence treatment of the wells with toxic chemical solutions, and the nonreusable specification of these products have driven the search for more efficient methods that can be tuned to the specific needs of individual laboratories. The technique introduced in this study is not only cost-effective, allowing for the reuse of the stamp straight after microwell formation, but this approach offers great tunability and flexibility for in-laboratory production of homogenous spheroids of multiple cell densities (up to 45,000 cells/spheroid) and cell sources (MSCs and ECs) compared with other existing tools. Furthermore, the use of agarose in the 3D printed stamps prevented MSC adherence to the microwell surface in comparison with the use of the Aggrewell plates, therefore increasing the efficiency of spheroid cell seeding. The depth and dimensions of the stamp-produced microwells avoided spheroid–spheroid fusion observed in the Aggrewell system. When compared with a mold method widely used in our laboratory,[24] spheroids produced using stamp-fabricated microwells were more homogeneous as shown by the reduced variability and lower standard deviation of the spheroid diameters. The *in situ* formation of the microwells within a tissue culture plate minimized the chance of infection by eliminating a transfer step, prevented the escape of seeded cells from the microwells, thus increasing the cell seeding efficiency, and ensured that all spheroids were located in the same spatial plane, thereby improving the facilitation of imaging and automated analysis and monitoring.

Microfabrication strategies have been widely used in the generation of nonadherent micropatterned surfaces as an alternative to the hanging drop method for the production of reproducible cell aggregates.[2,17,39,40] Most of these microfabrication techniques rely on the fabrication of a photosensitive epoxy resin master mold that is produced through photolithography. This master mold is subsequently used to generate a patterned PDMS[21,41–43] or silicone[20,21,41] elastomeric secondary mold that is used for the fabrication of nonadhesive microwells. Although these approaches allow for the precise patterning of microwells with a resolution in the nano- and micrometer range,[21] such techniques also involve a multistep, expensive, and time-consuming process requiring the use of toxic chemicals, high temperatures and pressures, and clean room facilities.[21]

More recently, the advent of 3D printing has facilitated the fast and cheap fabrication of precise 3D objects. In this study, a commercially available continuous liquid interface production[44] 3D printer was used to produce 24 stamps in a total printing time of 1 h. In addition, 3D printing offers high versatility for modification of the stamp characteristics in terms of material, size, and shape. As a result, 3D printing enables the rapid scaling up or down of the 3D object and the production of microwells in a diverse range of tissue culture plate sizes and shapes.

Conclusion

We demonstrate the potential of 3D printing for the fabrication of a tunable platform for spheroid production. This novel approach results in the reproducible patterning of microwells and the high-throughput production of cell spheroids. The developed technique could be adapted for a wide range of applications expanding from tissue engineering to the production of organoids for pharmacological and cancer research.

Disclaimer

The content is solely the responsibility of the authors and does not necessarily represent the official views of the National Institutes of Health.

Author Disclosure Statement

No competing financial interests exist.

Funding Information

This study was supported by the National Institutes of Health under Award No. R01 DE025475 to J.K.L. The funders had no role in the decision to publish, or preparation of the article. T.G.-F. received support from the American Heart Association Postdoctoral Fellowship (19POST34460034). A.J.T. received support from the UC Davis Provost's Undergraduate Fellowship (PUF) and the California Alliance for Minority Participation (CAMP) Scholarship.

References

1. Gionet-Gonzales MA, Leach JK. Engineering principles for guiding spheroid function in the regeneration of bone, cartilage, and skin. Biomed Mater 2018;13:034109.
2. Yin X, Mead BE, Safaee H, *et al.* Engineering stem cell organoids. Cell Stem Cell 2016;18:25–38.
3. Whitehead J, Zhang J, Harvestine JN, *et al.* Tunneling nanotubes mediate the expression of senescence markers in mesenchymal stem/stromal cell spheroids. Stem Cells 2020;38:80–89.
4. Hung BP, Harvestine JN, Saiz AM, *et al.* Defining hydrogel properties to instruct lineage-and cell-specific mesenchymal differentiation. Biomaterials 2019;189:1–10.
5. Ho SS, Hung BP, Heyrani N, *et al.* Hypoxic preconditioning of mesenchymal stem cells with subsequent spheroid formation accelerates repair of segmental bone defects. Stem Cells 2018;36:1393–1403.
6. Moldovan NI, Hibino N, Nakayama K. Principles of the kenzan method for robotic cell spheroid-based three-dimensional bioprinting. Tissue Eng Part B Rev 2017;23:237–244.
7. Quadrato G, Nguyen T, Macosko EZ, *et al.* Cell diversity and network dynamics in photosensitive human brain organoids. Nature 2017;545:48.
8. Fatehullah A, Tan SH, Barker N. Organoids as an in vitro model of human development and disease. Nat Cell Biol 2016;18:246.
9. Tuveson D, Clevers H. Cancer modeling meets human organoid technology. Science 2019;364:952–955.
10. Sasaki N, Clevers H. Studying cellular heterogeneity and drug sensitivity in colorectal cancer using organoid technology. Curr Opin Genet Dev 2018;52:117–122.
11. Harrison RG, Greenman M, Mall FP, *et al.* Observations of the living developing nerve fiber. Anat Rec 1907;1:116–128.
12. Sutherland RM, McCredie JA, Inch WR. Growth of multicell spheroids in tissue culture as a model of nodular carcinomas. J Natl Cancer Inst 1971;46:113–120.
13. Yuhas JM, Li AP, Martinez AO, *et al.* A simplified method for production and growth of multicellular tumor spheroids. Cancer Res 1977;37:3639–3643.
14. Costa EC, de Melo-Diogo D, Moreira AF, *et al.* Spheroids formation on non-adhesive surfaces by liquid overlay technique: Considerations and practical approaches. Biotechnol J 2018;13:1700417.
15. Huang JI, Kazmi N, Durbhakula MM, *et al.* Chondrogenic potential of progenitor cells derived from human bone marrow and adipose tissue: A patient-matched comparison. J Orthop Res 2005;23:1383–1389.
16. Souza GR, Molina JR, Raphael RM, *et al.* Three-dimensional tissue culture based on magnetic cell levitation. Nat Nanotechnol 2010;5:291.
17. Fennema E, Rivron N, Rouwkema J, *et al.* Spheroid culture as a tool for creating 3D complex tissues. Trends Biotechnol 2013;31:108–115.
18. Achilli T-M, Meyer J, Morgan JR. Advances in the formation, use and understanding of multi-cellular spheroids. Expert Opin Biol Ther 2012;12:1347–1360.
19. Tang MD, Golden AP, Tien J. Molding of three-dimensional microstructures of gels. J Am Chem Soc 2003;125:12988–12989.
20. Khademhosseini A, Eng G, Yeh J, *et al.* Micromolding of photocrosslinkable hyaluronic acid for cell encapsulation and entrapment. J Biomed Mater Res A 2006;79:522–532.
21. Qin D, Xia Y, Whitesides GM. Soft lithography for micro- and nanoscale patterning. Nat Protoc 2010;5:491.
22. Dahlmann J, Kensah G, Kempf H, *et al.* The use of agarose microwells for scalable embryoid body formation and cardiac differentiation of human and murine pluripotent stem cells. Biomaterials 2013;34:2463–2471.
23. Mehesz AN, Brown J, Hajdu Z, *et al.* Scalable robotic biofabrication of tissue spheroids. Biofabrication 2011;3:025002.
24. Vorwald CE, Ho SS, Whitehead J, *et al.* High-throughput formation of mesenchymal stem cell spheroids and entrapment in alginate hydrogels. Methods Mol Biol 2018;1758:139–149.
25. Williams PA, Silva EA. The role of synthetic extracellular matrices in endothelial progenitor cell homing for treatment of vascular disease. Ann Biomed Eng 2015;43:2301–2313.
26. Murphy KC, Whitehead J, Zhou D, *et al.* Engineering fibrin hydrogels to promote the wound healing potential of mesenchymal stem cell spheroids. Acta Biomater 2017;64:176–186.
27. Tevis KM, Cecchi RJ, Colson YL, *et al.* Mimicking the tumor microenvironment to regulate macrophage phenotype and assessing chemotherapeutic efficacy in embedded cancer cell/macrophage spheroid models. Acta Biomater 2017;50:271–279.
28. Birey F, Andersen J, Makinson CD, *et al.* Assembly of functionally integrated human forebrain spheroids. Nature 2017;545:54–59.
29. Liu J, Li R, Xue R, *et al.* Liver extracellular matrices bioactivated hepatic spheroids as a model system for drug hepatotoxicity evaluations. Adv Biosyst 2018;2:1800110.
30. Bartosh TJ, Ylöstalo JH, Mohammadipoor A, *et al.* Aggregation of human mesenchymal stromal cells (mscs) into 3D spheroids enhances their antiinflammatory properties. Proc Natl Acad Sci U S A 2010;107:13724–13729.
31. Bhang SH, Lee S, Shin J-Y, *et al.* Transplantation of cord blood mesenchymal stem cells as spheroids enhances vascularization. Tissue Eng 2012;18:2138–2147.
32. Wang W, Itaka K, Ohba S, *et al.* 3D spheroid culture system on micropatterned substrates for improved differentiation efficiency of multipotent mesenchymal stem cells. Biomaterials 2009;30:2705–2715.
33. Whitehead J, Kothambawala A, Leach JK. Morphogen delivery by osteoconductive nanoparticles instructs stromal cell spheroid phenotype. Adv Biosyst 2019;3:1900141.
34. Laib AM, Bartol A, Alajati A, *et al.* Spheroid-based human endothelial cell microvessel formation in vivo. Nat Protoc 2009;4:1202.
35. Vorwald CE, Murphy KC, Leach JK. Restoring vasculogenic potential of endothelial cells from diabetic patients through spheroid formation. Cell Mol Bioeng 2018;11:267–278.

36. Sutherland RM. Cell and environment interactions in tumor microregions: The multicell spheroid model. Science 1988;240:177–184.
37. Heiss M, Hellström M, Kalén M, *et al.* Endothelial cell spheroids as a versatile tool to study angiogenesis in vitro. FASEB J 2015;29:3076–3084.
38. Upreti M, Jamshidi-Parsian A, Koonce NA, *et al.* Tumor-endothelial cell three-dimensional spheroids: New aspects to enhance radiation and drug therapeutics. Transl Oncol 2011;4:365-IN363.
39. Rivron NC, Rouwkema J, Truckenmüller R, *et al.* Tissue assembly and organization: Developmental mechanisms in microfabricated tissues. Biomaterials 2009;30:4851–4858.
40. Liu T, Chien CC, Parkinson L, *et al.* Advanced micromachining of concave microwells for long term on-chip culture of multicellular tumor spheroids. ACS Appl Mater Interfaces 2014;6:8090–8097.
41. Kumar A, Biebuyck HA, Whitesides GM. Patterning self-assembled monolayers: Applications in materials science. Langmuir 1994;10:1498–1511.
42. Cho CH, Park J, Tilles AW, *et al.* Layered patterning of hepatocytes in co-culture systems using microfabricated stencils. Biotechniques 2010;48:47–52.
43. Sridhar A, de Boer HL, van den Berg A, *et al.* Microstamped petri dishes for scanning electrochemical microscopy analysis of arrays of microtissues. PLoS One 2014;9:e93618.
44. Tumbleston JR, Shirvanyants D, Ermoshkin N, *et al.* Continuous liquid interface production of 3D objects. Science 2015;347:1349–1352.

Address correspondence to:
J. Kent Leach
Department of Biomedical Engineering
University of California, Davis
451 Health Sciences Drive, 2303 GBSF
Davis, CA 95616
USA

E-mail: jkleach@ucdavis.edu